Bulletin of the Geological Society of Malaysia, Volume 58, December 2012, pp. 29 – 35

Characterizing and modeling natural fracture networks in a tight carbonate reservoir in the Middle East: A methodology

Dipak Singha Ray[1], Adnan Al-Shammeli[1], Naveen K. Verma[1], Saad Matar[1], Vincent de Groen[2], Ghislain de Joussineau[2], Laurent Ghilardini[2], Thierry Le Maux[2] & Waleed Al-Khamees[1]

[1] *Kuwait Oil Company, P.O Box 9758, Ahmadi, 61008 Kuwait*
[2] *Beicip-Franlab, 232 Avenue Napoleon Bonaparte, 92502 Rueil Malmaison, France*

Abstract: Fractured reservoirs are challenging to handle because of their high level of heterogeneity. In particular, natural fractures have a significant impact on well performance and water production. Therefore, understanding their significance through fracture characterization is helpful in well placement and field development.

This paper presents a best practice methodology for building a 3D stochastic fracture model using a Middle Eastern tight carbonate field example. This model is generated through the analysis and integration of data including cores, borehole images (BHI), logs, mud losses, production logs, well test data and 3D seismic data.

The impact of lithology on fracture occurrence was quantified based on rock-typing. Rock-types are distributed in a 3D geological model using a high resolution sequence stratigraphic framework. The length, dip angle and orientation of fractures, together with the shale content of the facies where they occur, were defined to sort the tectonic fractures from the non-tectonic (diagenetic) ones. It was found that multiple sets of tectonic diffuse fractures are generally associated with cleaner limestone units. Altogether, three sets of diffuse fractures were identified from BHI data: NE-SW, EW and NW-SE. In addition, large-scale fracture corridors, including sub-seismic faults identified from seismic analysis, were detected and calibrated with cores and BHI. The final model incorporates two scales of tectonic fractures with a direct bearing on field production behavior: diffuse fractures and large fracture corridors.

Fracture calibration was performed using production logs and well production data. Permeability at wells was computed in the 3D fracture model and matched with real build-up data. These data were then used to propagate 3D fracture properties (fracture porosity, fracture permeability and equivalent block size) in the upscaled geological model, for constructing a full-field reservoir simulation model. Few changes of the fracture properties were needed to obtain a good history match, indicating that the fracture model produced is robust.

Keywords: tight carbonate, fracture, DFN model, fracture porosity, fracture permeability

INTRODUCTION

Naturally fractured reservoirs are especially difficult to characterize, model and simulate because of high static and dynamic heterogeneity (Nelson, 2001; Narr *et al.*, 2006; Lonergan *et al.*, 2007). From a static point of view, the spatial variability of the fracture networks, frequently linked with variations of matrix properties, is a key parameter to assess. From a dynamic point of view, the high contrasts in flow behavior observed between wells should be understood in order to build predictive simulation models.

Because of the heterogeneous character of fractured reservoirs, any characterization study should imply the analysis and close integration of multi-scale data of various origins (Bourbiaux *et al.*, 2005). In this paper, we describe such an integrated approach, from geophysics to reservoir engineering, for the characterization and modeling of natural fracture networks occurring in a tight carbonate reservoir of a Kuwaiti field. In this Jurassic reservoir mainly composed of interbedded wackestone, packstone and mudstone facies, matrix porosity is typically lower than 3% and matrix permeability is typically lower than 1mD, stressing the importance of natural fracture networks on production.

Accordingly, the main challenge of the effort presented was to build a representative, multi-scale fracture model of the reservoir. This implied a correct assessment of the components of fracturing (large-scale fracture corridors, sets of small-scale diffuse fractures), their properties (fracture orientation, dip angle and density; fracture aperture and conductivity) as well and their possible variability. This was achieved through an integrated workflow combining the analysis of geological data (cores, borehole images (BHI), logs, rock-types), seismic data (horizons, faults, attributes) and dynamic data (mud losses, well tests, production and production logs). The main steps of the workflow followed include:

- Fracture characterization from cores
- Fracture characterization from BHI data
- Fracture characterization from seismic data
- Fracture characterization from dynamic data
- 3D Fracture modeling
- Dynamic calibration of fracture model
- Computation of full-field equivalent fracture properties

The final output of this fracture characterization and modeling effort was a set of fracture properties [(fracture porosity, fracture permeability (Kx, Ky, Kz) and matrix bloc size (a, b, c)] computed in each cell of the simulation grid. Such fracture parameters are uncertain and usually very difficult to assess, but are obtained in our methodology as an output of an integrated study whereas many other simulations require them as input parameters.

In a next step of dual-medium simulation, satisfying history match was reached with only minor adjustments of the fracture properties computed, showing the accuracy and adequacy of the fracture study carried out.

FRACTURE CHARACTERIZATION

In this task, the key objectives were to identify the types of natural fractures occurring in the reservoir, understand their distribution and assess their possible impact on fluid flow. The methods used and the results obtained are detailed hereafter.

Core analysis

Cores were available in 4 wells in the studied field and 9 wells in nearby fields. Their analysis revealed the existence of two main types of natural fractures in the reservoir units (Figure 1):

1. Early-diagenetic fractures, related to processes occurring during the transformation of sediments into rocks (compaction, dessication, dolomitization,…)
2. Tectonic fractures, related to the deformation of cohesive rocks under stress

Early-diagenetic fractures are characterized by small dimensions and frequent calcite cementation (Figure 1a). These characteristics suggest that they could not have an important impact on fluid flow and, as such, that they should not be included in fracture models of the reservoir.

On the other hand, tectonic fractures were frequently observed, with large dimensions and no or partial cementation (Figure 1b). These attributes suggest a possible important impact on fluid flow, indicating that tectonic fractures are the natural fractures to be represented in fracture models of the reservoir.

A final critical observation made on cores is that tectonic fractures occur only in clean limestone units, for which the volume of shale is less than 20% (Figure 1c). This impact of lithology on fracture occurrence provided important information for controlling the spatial distribution of tectonic fractures in the 3D fracture model of the reservoir.

Bore Hole Image (BHI) analysis

Eight wells with resistivity and/or acoustic image logs were available for the study. Their interpretation was controlled and only the fractures considered as high- or medium-confidence features, based on the continuity of their traces on the images, were used for the analysis. In addition, the few fractures observed in shaly units (VSH>20%), considered as early-diagenetic fractures based on core observations (Figure 1c), were discarded for analysis.

In a first step, the fracture data from all wells were analyzed together in order to identify the main fracture orientations in the reservoir. The population of tectonic fractures identified on BHI data is organized along three clear trends: a dominant NE-SW trend and two, secondary EW and NW-SE trends (Figure 2).

In a second step, once the main fracture orientations identified, a detailed analysis of fracture distribution was carried out in order to separate small-scale diffuse fractures (small, bed-bounded fractures organized in sets with moderate variations of orientation within one set, with large geographic distribution and usually controlled by matrix properties) from large-scale fracture corridors (features with high lateral and vertical dimensions, distributed in localized areas and independent of matrix properties). These two fracture components have different signature on the fracture density logs computed at wells based on BHI data.

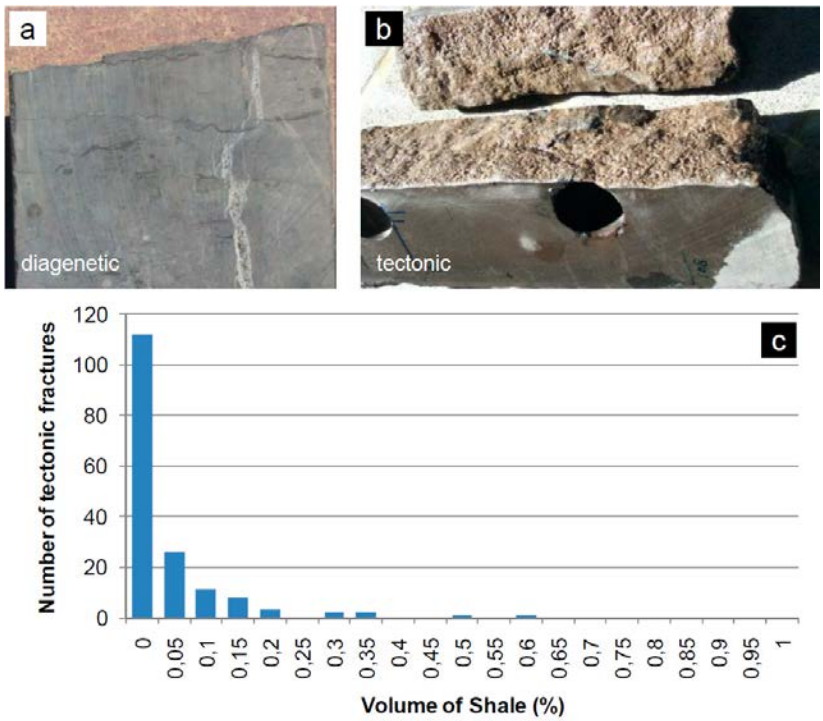

Figure 1: (a) Example of diagenetic fracture; (b) example of tectonic fracture; (c) distribution of tectonic fractures in cores as a function of the volume of shale.

Diffuse fractures usually show moderate values of fracture density and several sets typically occur at the same depth, resulting in different fracture orientations observed in the same well interval (Figure 3a). In contrast, fracture corridors are detected by localized peaks on fracture density logs, with all fractures sharing the same orientation (Figure 3b). Using these contrasting attributes of diffuse fractures and fracture corridors, the fracture types were separated and the statistical properties of each fracture type, critical for further fracture modeling, were computed (Figure 4a, example for diffuse fractures; Figure 4b, example for fracture corridors). Fracture density was computed taking into account the angle between the fractures planes and the well path.

Finally, the relationships between lithology and fracture distribution observed during the core analysis were tested by comparing the logs of diffuse fracture density at wells with other logs related to matrix properties (e.g. VShale, porosity,..) and the rock types defined during a prior phase of geological modeling. This allowed confirming the impact of lithology on diffuse fracture distribution and computing an average diffuse fracture density value per rock type (Figure 4c), to be used for diffuse fracture modeling.

Fracture analysis from seismic

In this section, the seismic data (top reservoir horizon, faults and seismic attributes) were used to complete the detection of seismic faults by the identification and mapping of sub-seismic faults (or fracture lineaments) which are expected to form fracture corridors.

In a first step, a seismic facies analysis study was carried out (Abdul *et al.*, 2010), which allowed producing maps of fractured seismic facies and normalized seismic fracture density (Figure 5a). These maps give precious information about the large-scale fracturing affecting the reservoir.

In a second step, the seismic fracture maps and a series of maps of seismic attributes such as coherency or edge were combined with a curvature analysis (Stewart & Podolski, 1998) performed on the top reservoir horizon. This approach allowed the validation and extension of the seismic faults, and the detection of many new fracture lineaments (Figure 5b). These lineaments have NE-SW, NW-SE and EW orientations, consistent with seismic fault orientations and fracture orientations observed in the wells.

The new complete fault map of Figure 5b shows all of the large fracture corridors occurring in the reservoir, and served as a basis for the modeling of such features.

Fracture Characterization using dynamic data

In this section, the possible impact of fractures on fluid flow was analyzed using all available dynamic data (production and pressure, flowmeters, transient tests and mud losses) for 12 wells of the studied reservoir.

A complete series of analyses was carried out in order to (1) find evidence of fractures impacting the fluid flow, (2) determine whether this impact was positive or negative and (3) determine the scale of fractures involved (diffuse fractures, fracture corridors or both). This approach was based on a close integration with static data (BHI and seismic).

An example of analysis carried out is shown in Figure 6. In this figure, the presence of fractures in one well is compared with the occurrence of mud losses. A very good relationship is observed, clearly showing the positive impact of fractures on production.

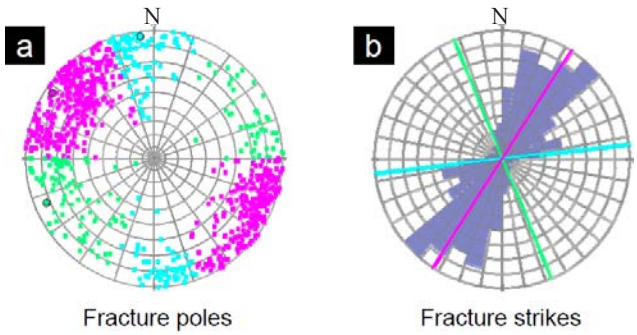

Figure 2: Fracture poles (a) and corresponding fracture strikes (b) allowing to define 3 fracture sets oriented NE-SW, EW and NW-SE in the reservoir.

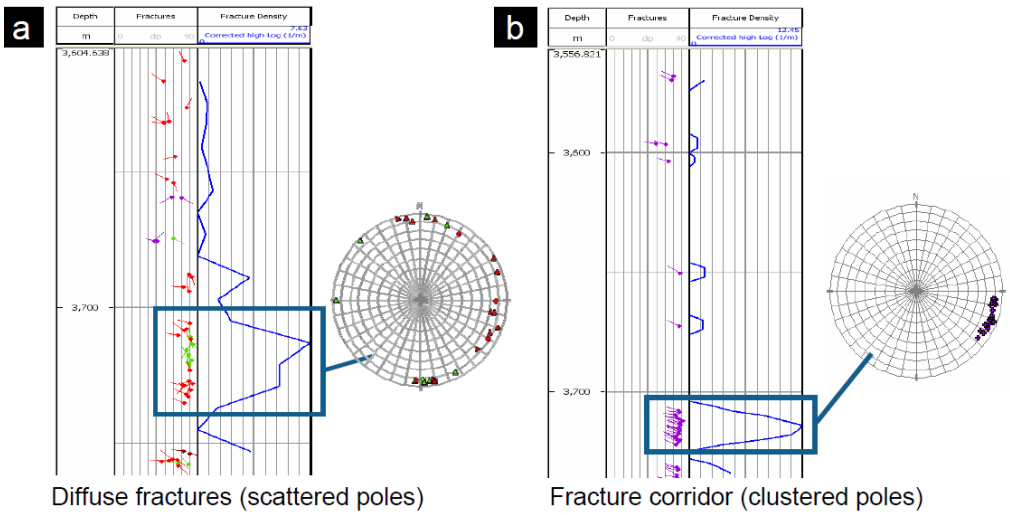

Figure 3: Example of signature of diffuse fractures (a) and a fracture corridor (b) on fracture density logs.

Another important analysis included calculating the ratio between the KH obtained from the well test interpretations and the KH calculated from cores (or permeability logs if no sufficient core data were available). This ratio is an estimate of the ratio between the KH of both the fractures and matrix together (well test measurement) and the KH of the matrix (core measurement). It is a good indicator of the contribution of fractures to flow, especially if the KH ratio is greater than 10 (Narr *et al.*, 2006). A ratio of 1135 was computed in one of the wells, indicating that fractures play a major role in the fluid flow in the reservoir.

The results of all of the dynamic analyses were synthesized. Overall, 8 main criteria were used for identifying the impact of fractures on production:

1. A high fracture density observed on BHI
2. A high KH value from well test
3. A high KH ratio between test and core measurements
4. An indication of fracture (here, sealing fault) on the well test signatures
5. An anomaly in the production logs
6. An early water breakthrough at the wells
7. The occurrence of mud losses
8. A high flow rate

Not all data were available in all wells but the results obtained throughout the field were sufficiently consistent to identify (1) a clear positive effect of all fracture types on fluid flow (fractures contributing to production) and (2) a role of seal for cross-fault fluid flow played by the large faults (from well test signatures).

3D fracture modeling

Once the fracture characterization was completed, the information obtained in terms of the components of fracturing, their distribution in the reservoir units and their possible dynamic impact were used in order to build a 3D fracture model using an advanced fracture modeling methodology (Bourbiaux *et al.*, 2005).

As seen during the fracture characterization phase, two types of tectonic fractures occur in the reservoir units and should be represented in the DFN (Discrete Fracture Network) model: small-scale diffuse fractures with NW-SE, NE-SW and EW orientations, and large-scale fracture corridors.

The diffuse fractures were generated using an object-oriented stochastic process described by Cacas *et al.* (2001), based on the relationship between rock types and diffuse fracture density established in this study. The mean orientation in the fracture sets was interpolated in the 3D grid from values at wells and a fixed standard deviation was assigned by fracture set based on wells results. Fracture length was considered to obey a power law distribution, as observed for larger-scale fracture corridors. The mean fracture length was set to 20 m and the minimum and maximum length values to 3 m and 50 m, respectively. These values are consistent with field observations of fracture networks (de Joussineau & Aydin, 2007). The diffuse fractures were bounded by sub-layers created in each cell of the 3D grid. The DFN model built was controlled in order to check the expected behavior in terms of fracture density and connectivity, with a dominant NE-SW fracture set and two secondary NW-SE and EW fracture sets (Figure 7a).

The modeling of large-scale fracture corridors was based on the interpretation of faults in seismic and the detection and mapping of fracture lineaments derived from curvature analysis and seismic facies analysis. The position and geometry of the seismic faults and fracture lineaments were used to create fracture corridors in the reservoir. These corridors were represented as vertical features crosscutting all of the layers of the reservoir grid (Figure 7b).

Dynamic calibration of fracture model

Once built, the fracture model of the reservoir was calibrated in terms of hydraulic properties of the fractures (conductivity and aperture) using the KH values obtained from well tests in three representative wells of the field.

To do so, local fracture models were first built around the three wells, in the estimated region of investigation of the well tests (Figure 8a). Second, a geologically reasonable value was set for the conductivity of the different fracture components (sets of diffuse fractures and fracture corridors), and the equivalent KH values of the models were computed (Figure 8b). These calculated KH were compared to the ones given by the well test interpretations, and the conductivities of the fracture components were adjusted until a good match was reached. This calibration provided conductivity values of 66 mD.ft for the diffuse fractures and of 90000 mD.ft for the fracture corridors. Finally, fracture apertures were derived from the calibrated conductivities using the Poiseuille's law:

$$Cf = \frac{e^3}{12 * 0.98.10^{-6}} \quad (1)$$

where Cf is the fracture conductivity in mD.m and e is the fracture aperture in mm. The fracture apertures were found equal to $2.03\ 10^{-4}$ ft for diffuse fractures and $13.1\ 10^{-2}$ ft for fracture corridors.

Computation of full-field equivalent fracture properties

Once the hydraulic properties of fractures calibrated in the DFN model, the ultimate task was to compute full-field, equivalent properties of the fracture networks to be used in dual-medium simulations. This task consisted in converting a geological image of the reservoir, the DFN model with its complex fracture network architecture, into a simplified dual-porosity model. This simplified conceptual model, representing the fractured reservoir as an array of parallelepipedic matrix blocks limited by a set of uniform orthogonal fractures, was introduced by Warren & Root (1963).

The required equivalent fracture parameters for the dual-porosity simulation are the equivalent permeability (in X, Y and Z), the equivalent porosity and the equivalent matrix block size (in X, Y and Z). In this study, the equivalent fracture parameters were computed from an upscaling of

a

Wells	Sets of diffuse fractures	Data	
Well A	NE-SW	number of fractures	51
		mean strike	N44E
		mean dip angle	81°
		mean density (f/m)	0.35
	NW-SE	number of fractures	31
		mean strike	N148E
		mean dip angle	70°
		mean density (f/m)	0.21
	EW	number of fractures	20
		mean strike	N90E
		mean dip angle	80°
		mean density (f/m)	0.15

b

	Cluster	C1	C2	C3	C4	C5
Well A	MD interval (m)	3876-79	3894-96	3992-93	4000-02	4013-17
	number of fractures	7	5	5	7	8
	mean strike	N158E	N172E	N42E	N50E	N08E
	mean dip angle	72°	70°	83°	88°	70°
	mean density (f/m)	2.9	2.97	3.59	4.07	2.36

c

Rock type	Average diffuse fracture density (f/m)
#1	0.00
#2	0.33
#3	0.16
#4	0.18
#5	0.23
#6	0.23
#7	0.13

Figure 4: (a) Example of statistics of diffuse fractures in one well; (b) example of statistics of fracture corridors in the same well; (c) diffuse fracture density per rock type.

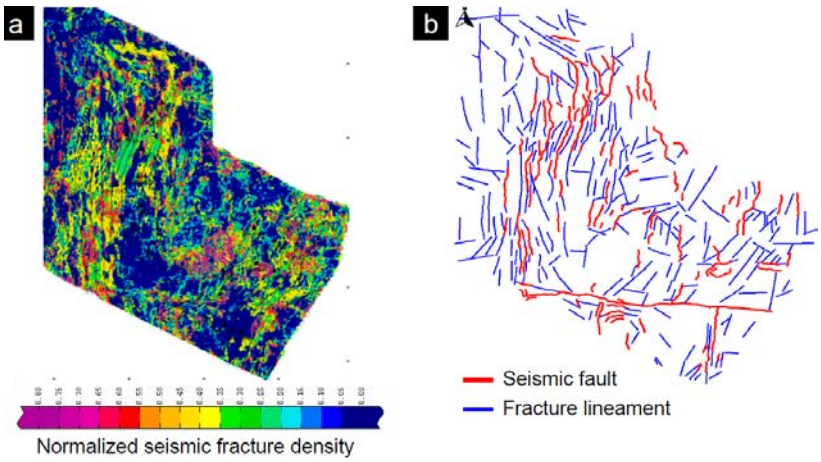

Figure 5: (a) Seimic fracture density map obtained from the seismic facies analysis and used to finalize the detection of faults; (b) final fault map at the top of the reservoir.

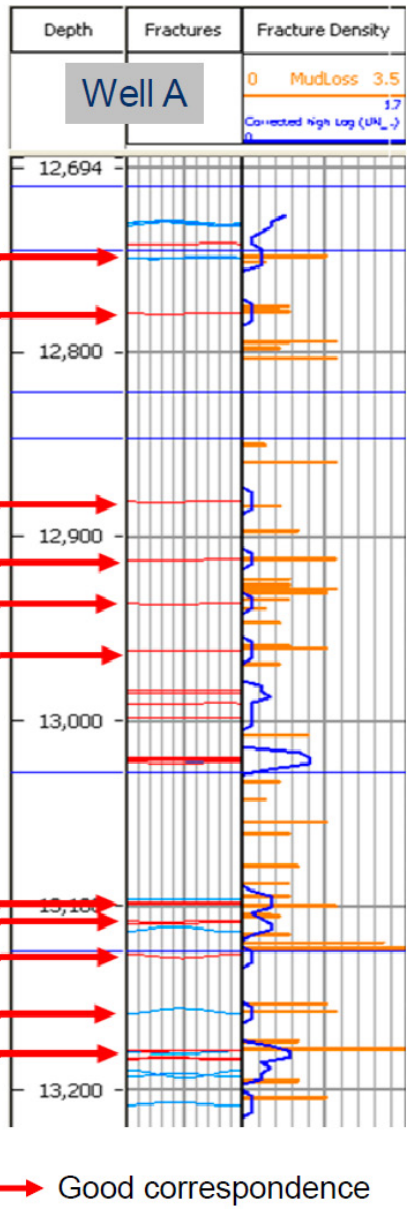

Figure 6: Clear relationships between mud loss occurrences and the presence of fractures in the reservoir in well A.

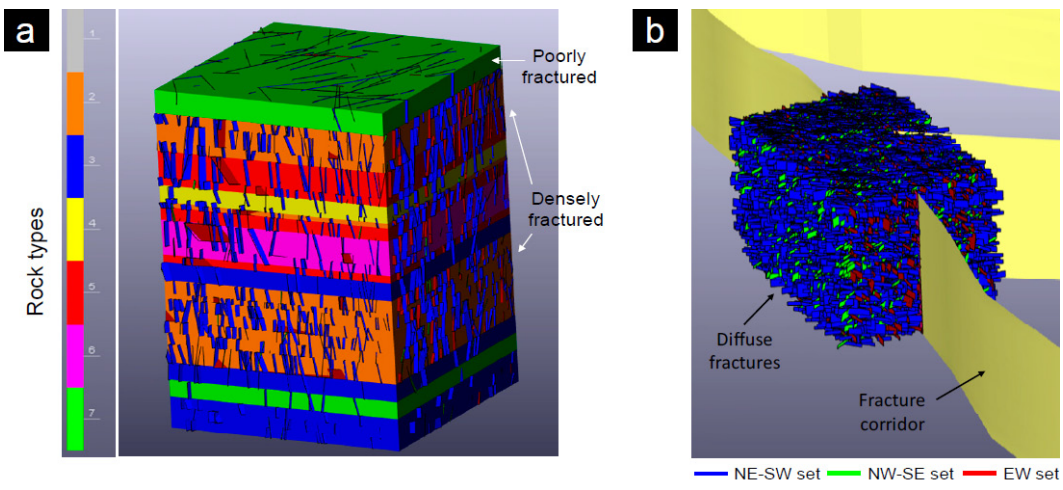

Figure 7: (a) Example of DFN model for diffuse fractures, showing the control of rock types on fracture density; (b) example of DFN model with both diffuse fractures (bed-bounded) and fracture corridors (crosscutting all reservoir units).

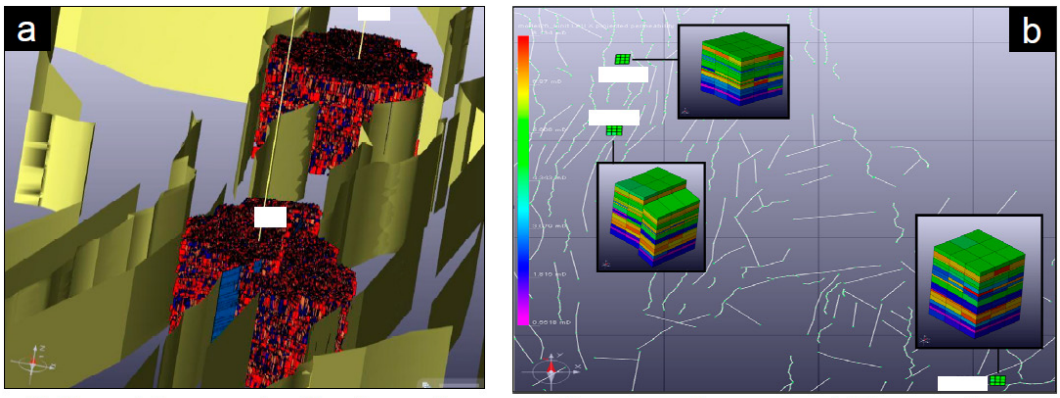

Figure 8: Local DFN models around calibration wells (a) and corresponding permeability computation (b).

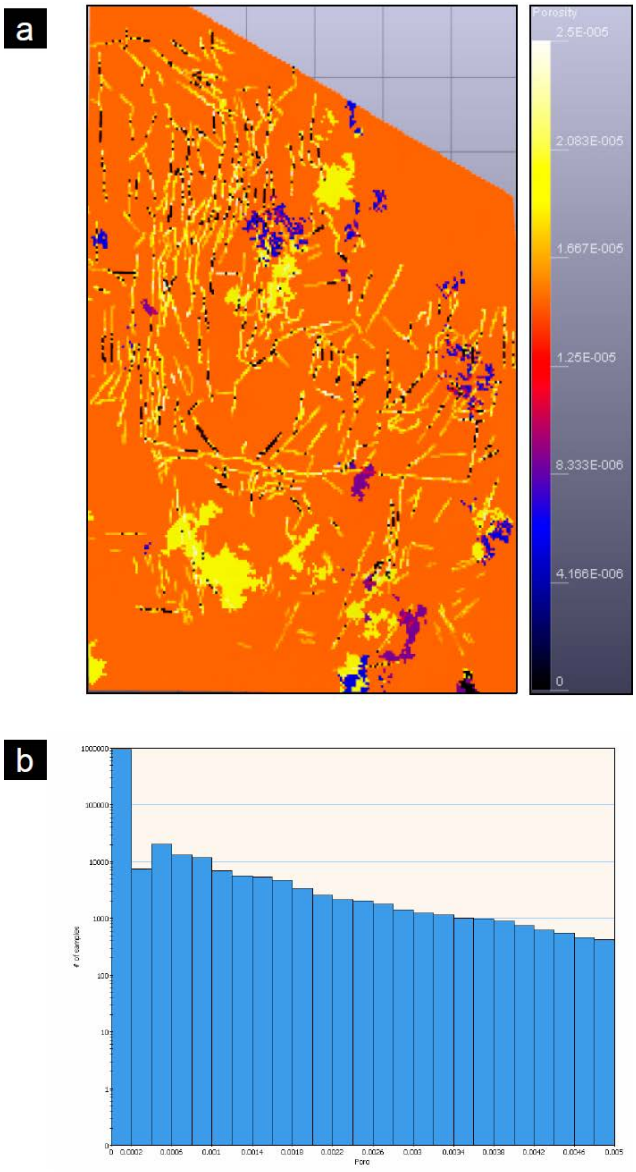

Figure 9: (a) Fracture porosity map at the top of the reservoir; (b) Frequency distribution of fracture porosity values in the model.

the fracture model by using an analytical method (Oda, 1985). For the diffuse fractures, the permeability in X and Y directions is ~ 4 mD (with variations related to the fracture density variations between the rock types), the permeability in Z direction is ~ 20 mD and the porosity is ~ 0.002%. For the fracture corridors, the permeability in X and Y directions is ~ 300 mD, the permeability in Z direction is ~ 20 D and the porosity is ~ 0.2%. Finally, the matrix block sizes are ~ 3 m horizontally and 9 m vertically. Figure 9 illustrates these results by showing the fracture porosity at the top of the reservoir (Figure 9a) and the distribution of fracture porosity values in the model (Figure 9b).

These equivalent fracture properties formed the basis for taking into account the critical role of natural fractures on fluid flow in the reservoir units during a next phase of dual-medium simulation. A good history match of the production data was reached with only minor adjustments of these fracture properties (Figure 10), suggesting the adequacy and robustness of the fracture model developed.

CONCLUSIONS

A robust methodology for multi-scale fracture characterization and modeling is presented, which integrates geophysics, geology and reservoir engineering disciplines. It was successfully applied to a tight carbonate reservoir of the Middle-East (matrix with typically less than 3% porosity and 1 mD permeability), in which accurate fracture characterization and modeling is key to predictive dynamic simulations.

Cores, borehole images and seismic were used to identify the components of fracturing occurring in the reservoir, and to characterize their distribution. Fracturing consists of three sets of small-scale diffuse fractures with NE-SW, NW-SE and EW orientations, and large-scale fracture corridors. The distribution of diffuse fractures is a function of matrix properties, and a relationship between diffuse fracture density and rock types was established.

The analysis of dynamic data, in close integration with the static data, identified a clear positive effect of fractures on production, along with the sealing character of large faults for cross-fault fluid flow.

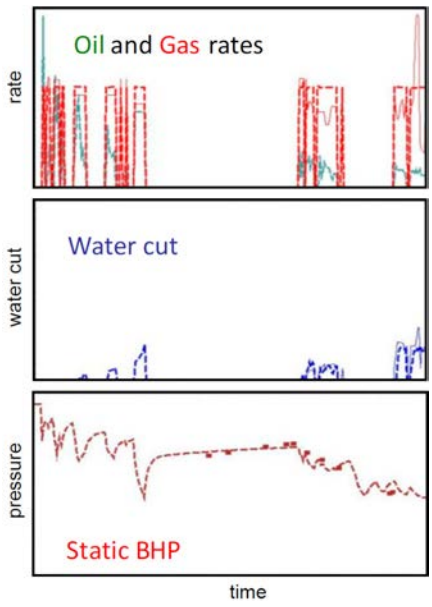

Figure 10: Example of final history-match (oil and gas rates, water cut and static bottom-hole pressure) in one well. Modeled curves are dashed.

All of the results obtained during the fracture characterization phase were integrated in order to build a representative DFN (fracture) model of the reservoir, which was calibrated with well test data. Finally, full-field equivalent fracture properties were computed and used in a next phase of dual-medium dynamic simulation. A good history match was reached with only minor adjustments of fracture properties. This indicates the accuracy and adequacy of the fracture characterization and modeling work carried out.

ACKNOWLEDGMENTS

The authors would like to thank the management of the Kuwait Oil Company (KOC) for permission to publish this paper, Bernard J. Pierson and Adriaan Bal for thoughtful reviews.

REFERENCES

Abdul, J.A., Matar, S., Convert, P., Rocher, D., & de Groen, V., 2010. Seismic characterization for stochastic modeling of fractures in NJ-SR reservoirs of UG Field, West Kuwait. Oral presentation #681063, Geo2010 Conference, Kingdom of Bahrain.

Bourbiaux, B., Basquet, R., Daniel, J.M., Hu L.Y., Jenni, S., Lange, A., & Rasolofosaon, P., 2005. Fractured reservoirs modelling: a review of the challenges and some recent solutions. First Break, 23, 33-40.

Cacas, M.C., Daniel, J.M., & Letouzey, J., 2001. Nested geological modelling of naturally fractured reservoirs. Petroleum Geoscience, 7, S43-S52.

de Joussineau, G., & Aydin, A., 2007. The evolution of the damage zone with fault growth in sandstone and its multiscale characteristics. Journal of Geophysical Research, 112, B12, B12401, 10.1029/2006JB004711.

Lonergan, L., Jolly, R.J.H., Rawnsley, K., & Sanderson, D.J., 2007. Fractured reservoirs. Geological Society Special Publication 270, London. 285p.

Narr, W., Schechter, D.W., & Thompson, L.B., 2006. Naturally fractured reservoir characterization. Society of Petroleum Engineers. 115p.

Nelson, R., 2001. Geologic analysis of naturally fractured reservoirs. Elsevier. 352p.

Oda M., 1985. Permeability tensor for discontinuous rock masses. Géotechnique, 35, 483-495.

Stewart, S.A., Podolski, R., 1998. Curvature analysis of gridded geological surfaces. In: Coward, M.P., Daltaban, T.S. and Johnson, H. (Eds.), Structural Geology in Reservoir Characterization. Geological Society Special Publication 127, London, pp. 133-147.

Warren J.E., & Root, P.J., 1963. The behavior of naturally fractured reservoirs. Society of Petroleum Engineers Journal, 228, 245-255.

Manuscript received 20 Sep 2011
Revised manuscript received 27 Aug 2012